**substance: boron compounds with group II elements**
**property: properties of boron-magnesium compounds**

On the structure of thermal magnesium boron [91T].

Theoretical conclusion that a Mg atom can be accommodated within a $B_{12}$ icosahedron in [86B1, 87B].

**$MgB_2$**

metallic conduction (?); preparation [75S], crystalline structure [75S, 77C], electronic structure [77P, 77C]

Entropy in [86B2].

**$MgB_4$**

preparation [75S, 72G, 77N]; crystalline structure [72G, 77N]

Entropy in [86B2].

**$MgB_6$**

semiconductor (?); preparation [75S]; crystalline structure [75S], electronic structure [77P, 77E]

**$MgB_{12}$**

preparation [75S]; crystalline structure [75S]

**entropy**

| | | |
|---|---|---|
| *S* | 89.52 J $mol^{-1}$ $K^{-1}$ | 86B2 |

**$Mg_2B_{14}$**

semiconductor (?); preparation [81G, 70M]; crystalline structure [81G, 76N, 70M, 70E]

Structure: orthorhombic

Space group: Imam

The structure contains five independent boron and two independent Mg atoms.

**lattice parameters**
(in Å)

| | | | | |
|---|---|---|---|---|
| *a* | 5.970 | *T* = 300 K | X-ray diffraction | 81G |
| *b* | 8.125 | | | |
| *c* | 10.480 | | | |

**occupation of Mg sites**

| | | | |
|---|---|---|---|
| Mg(1) | 93(1.5) % | *T* = 300 K | 81G |
| Mg(2) | 100 % | | |

Comparison of the interatomic distances in $Mg_2B_{14}$ with $LiAlB_{14}$, $MgAlB_{14}$ and $NaB_{0.8}B_{14}$ in [81H].

**$MgAlB_{14}$**

**Structure**

The structure (Fig. 1) can be considered as being constituted of distorted, closest-packed layers of quasi-spherical icosahedra stacked directly one above the other in the *c*-direction [65M, 70M, 77M1, 77M2]. Another description is based on chains of $B_{12}$ icosahedra running in the *c*-direction. In a chain, the icosahedra are orientated in such a way that one of their mirror planes is parallel to the bc-plane, one of their pseudo fivefold axes being alternately inclined 7.88° to the *c*-axis [76N]. The chains are linked either by direct inter-icosahedral B – B bonds or by bridges involving isolated B atoms. The metal atoms partially occupy interstitial holes in the boron network.

**space group:** $D_{2h}^{28}$ – Imam.

**lattice parameters**
(in Å)

| | | | | |
|---|---|---|---|---|
| *a* | 5.848(1) | *T* = 300 K | X-ray diffraction | 93W, |
| *b* | 8.112(1) | | | 87H, |
| *c* | 10.312(1) | | | 83H, |

| | | | | |
|---|---|---|---|---|
| | | | | 93H |
| *a* | 5.858 | | $Mg_{0.5}AlB_{14}$ | 70M, |
| *b* | 8.115 | | | 76N, |
| *c* | 10.313 | | | 77M1 |

**interatomic distances**
(in Å)

| | | | |
|---|---|---|---|
| *d* | 2.27 | Al – 12B | 93W |
| | 2.70 | Mg – 16B | |
| | 2.924 | Al – Al | |
| | 3.07/3.41/3.74 | Li – Li | |

Comparison of the interatomic distances in $MgAlB_{14}$ with $LiAlB_{14}$, $Mg_2B_{14}$ and $NaB_{0.8}B_{14}$ in [81H].

**occupancies and positions of the metal atoms**
(data from [77M2])

| Atoms | Position | Coordinates | | | Occupancies |
|---|---|---|---|---|---|
| | | *x* | *y* | *z* | |
| $M_1$ | 4(e) | – 0.359 | 1/4 | 1.205 | Al: 25; Mg: 50 |
| $M_2$ | 4(d) | 1/4 | 1/4 | 1/4 | Al: 75 |

**Physical properties**

**energy gaps**
(in eV)

| | | | | |
|---|---|---|---|---|
| $E_g$ | 0.27 | | $E_F - E_V$ | 87G |
| | | | estimated from el. cond., pure material | |
| | 0.47 | | estimated from el. cond., Ni-doped mat. | 83G |
| | 0.16(1) | $T$ = 300 K | optical absorption, deep level to band | 93W |
| | 0.63(1) | | optical absorption, deep level to band | |
| | 0.99(3) | | indirect allowed interband | |
| | | | with phonon emission | |
| | 1.51(1) | | indirect allowed interband | |
| | | | with phonon emission | |

Optical absorption spectra of $MgAlB_{14}$ (compared with $LiAlB_{14}$ and $ErAlB_{14}$) in particular in the range of the absorption edge in Fig. 2 [93W]. See also [94W].

Optical reflectivity spectrum of $MgAlB_{14}$ (compared with $LiAlB_{14}$) in Fig. 3 [93W].

Optical absorption spectra of $MgAlB_{14}$ (compared with $LiAlB_{14}$ and $ErAlB_{14}$) in the range of the phonon frequencies in Fig. 4 [93W]. See also [87H, 94W].

**electrical conductivities**
(polycrystalline samples)

| | | | | |
|---|---|---|---|---|
| $\sigma$ | $2 \cdot 10^{-1}\ \Omega^{-1}\ cm^{-1}$ | $T$ = 300 K | pure $MgAlB_{14}$ (see also Fig. 5) | 79B |
| | $5 \cdot 10^{-2}\ \Omega^{-1}\ cm^{-1}$ | | Ni-alloyed | 79B |
| | $2 \cdot 10^{-4} \Omega^{-1} cm^{-1}$ | $T$ = 300 K | | 94W |

Temperature dependence of the electrical conductivity of pure and Fe-doped $MgAlB_{14}$ in Fig. 6 [89K].

**thermoelectric powers**
(polycrystalline samples)

| | | | | |
|---|---|---|---|---|
| $S$ | 260 μV $K^{-1}$ | $T$ = 400 K | pure $MgAlB_{14}$ (see also Fig. 7) | 79B |
| | 230 μV $K^{-1}$ | | Ni-alloyed | 79B |
| | –6300 μV $K^{-1}$ | $T$ = 300 K | | 94W |
| | 400 μV $K^{-1}$ | $T$ = 300 K | | 94G |

Thermoelectric power dependence on Hall concentration in Fig. 8 [83G, 87G].

Temperature dependence of the thermoelectric power of pure and Fe-doped $MgAlB_{14}$ in Fig. 9 [89K].

**density**

| | | | |
|---|---|---|---|
| $d$ | 2.585 g $cm^{-3}$ | $Mg_{0.5}AlB_{14}$, calculated | 70M |
| | 2.60 g $cm^{-3}$ | experimental | 76N |

**microhardness**

| | | | |
|---|---|---|---|
| $H_K$ | 2790...2890 kg $mm^{-2}$ | (001) | 93H |

**melting point**

| | | | |
|---|---|---|---|
| $T_m$ | ~2300 K | estimated | 81H |

### Doped $MgAlB_{14}$

On the structure of thermal magnesium boron [91T].

Electrical conductivity, Seebeck effect and Moessbauer effect of Fe-doped $MgAlB_{14}$ see Fig. 9 [89K].

From a Mössbauer spectrum [94G] was concluded that $Fe^{3+}$ substitute for Mg and $Fe^{2+}$ for Al atoms in the structure.

**thermoelectric power**
(in μV $K^{-1}$)

| | | | | |
|---|---|---|---|---|
| $S$ | 400 | $T$ = 300 K | undoped | 94G |
| | 230 | | 0.5 at. % Fe | |
| | 10 | | 2 at. % Fe | |
| | 42 | $T$ = 360 K | Ni doped (conc. not specified) | 83G |

Temperature dependence of conductivity and thermoelectric power of Ni-doped $MgAlB_{14}$ in Fig. 10 [83G].

Temperature dependence of thermoelectric power (undoped, compared with 0.5 at. %, and 2 at-.% Fe-doped) in Fig. 11 and Fig. 9 [94G].

## References:


65M Matkovich, V. I., Giese, R. F., Economy, J.: Z. Kristallogr. 122 (1965) 66.

70E Boron 3, T. Niemyski, ed., PWN Warsaw, 1970

70M Matkovich, V. I., Economy, J.: Acta Crystallogr. B 26 (1970) 616.

70W Will, G.: see [70E], p. 119.

72G Guette, A., Naslain, R., Gaily, J.: C. R. Acad. Sci. Colon. Ser. C 275 (1972) 41.

75S Samsonov, G. V., Serebryakova, T. I., Neronov, V. A.: Boridy, Moskva Atomizdat, 1975.

76N Naslain, P., Guette, A., Hagenmuller, P.: J. Less-Common Met. 47 (1976)1.

77B Berezin, A. A., Golikova, O. A., Zaitsev, V. R., Kazanin, M. M., Orlov, V. M., Tkalenko, E. N., in:Boron and Refractory Borides, (Matkovich V. 1., ed.) Springer: Berlin, Heidelberg, New York 1977, p. 52.

77C Castaing, J., Costa, P.: see [77B], p. 390.

77E Etourneau, J., Mercuno, J. P., Hagenmuler, P.: see [77B], p. 115.

77M1 Matkovich, V. I., Economy, J.: see [77B], p. 78.

77M2 Matkovich, V. I., Economy, J.: see [77B], p. 96.

77N Naslain, R.: see [77B], p. 139.

77P Perkins, P. G.: see [77B], p. 31.

79B Bairamashvili, I. A., Kekelidze, L. I., Golikova, O. A., Orlov, V. M.: J. Less-Common Met. 67 (1979) 461.

81A Armstrong, D. R.: Proc. 7th Int. Symp. Boron, Borides and Related Compounds. Uppsala, Sweden, 1981; spec. issue of J. Less-Common Met. 82 (1981) 357.

81G Guette, A., Barret, M., Naslain, R., Hagenmuller, P., Tergenius, L. F., Lundström, T.: see [81A], p. 325.

81H Higashi, I.: J. Less-Common Met. 82 (1981) 317.

83A Armstrong, D. R., Bolland, J., Perkins, P. G. . Will, G. . Kirfel, A.: Acta Crystallogr. B39 (1983) 324.

83G Golikova, O.A., Samatov, S.: Phys. Status Solidi (a) 77 (1983) 449.

83H Higashi, I., Ito, T.: J. Less-Common Met. 92 (1983) 239.

86B1 Beckel, C.L., Howard, I.A.: Chem Phys. Lett. 130 (1986) 254.

86B2 Borovikova, M.S., Fesenko, V.V.: J. Less-Common Met. 117 (1986) 287. ( Proc. 8th Int. Symp. Boron, Borides, Carbides, Nitrides and Rel. Compounds, Tbilisi, Oct. 8 - 12, 1984)

87B Beckel, C.L., Howard, I.A.: in: Proc. 9th Int. Symp. Boron, Borides and Rel. Compounds, University of Duisburg, Germany, Sept. 21 - 25, 1987, H. Werheit ed., University of Duisburg: Duisburg, 1987, p. 263.

87G Golikova, O.A.: Phys. Status Solidi (a) 101 (1987) 277.

87H Haupt, H., Werheit, H., Siejak, V., Kannengiesser, U., Higashi, I.: in: Proc. 9th Int. Symp. Boron, Borides and Rel. Compounds, University of Duisburg, Germany, Sept. 21 - 25, 1987, H. Werheit ed., University of Duisburg: Duisburg, 1987, p. 385.

89K Kazanin, M.M., Kutasov, V.V.: Phys. Status Solidi A 113 (1989) 143.

91T Tkachev, K.V., Kerkher, T.E., Knyshev, E.A., Kogan, B.S., Plyshevskii, E.A.: AIP Conf. Proc. 231 (1991) 255in: Boron-Rich Solids (AIP Conf. Proc. 231), Albuquerque, New Mexico 1990, D. Emin, T. Aselage, A.C. Switendick, B. Morosin and C.L. Beckel ed., American Institute of Physics: New York, 1991, p. 255.

93H Hori, A., Kimura, K., Tada, T., Yamashita, H.: J. Non-Cryst. Solids 153&154 (1993) 308.

93W Werheit, H., Kuhlmann, U., Krach, G., Higashi, I., Lundström, T., Yu, Y.: J. Alloys Compounds 202 (1993) 269.

94G Golikova, O.A., Higashi, I.: Proc. 11th Int. Symp. Boron, Borides and Rel. Compounds, Tsukuba, Japan, August 22 - 26, 1993, Jpn. J. Appl. Phys. Series 10 (1994), p. 52.

94W Werheit, H., Krach, G., Kuhlmann, U., Higashi, I., Lundström, T., Yu, Y.: Proc. 11th Int. Symp. Boron, Borides and Rel. Compounds, Tsukuba, Japan, August 22 - 26, 1993, Jpn. J. Appl. Phys. Series 10 (1994), p. 98.

**Fig. 1.**

$MgAlB_{14}$. A layer of icosahedra with extra-icosahedral atoms. The atoms with $-1/4 \leq x \leq +1/4$ are represented [77M2].

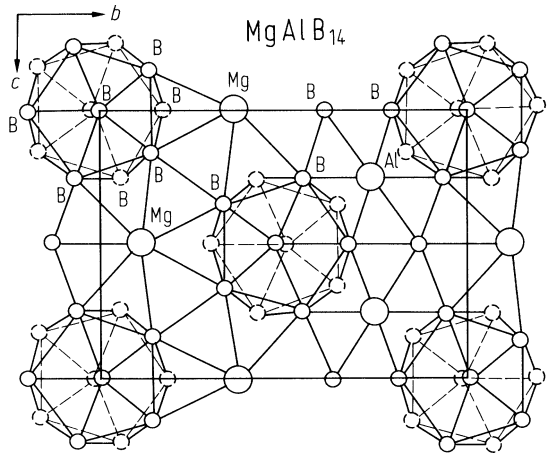

**Fig. 2.**

$MgAlB_{14}$ type orthorhombic structure group ($LiAlB_{14}$, $MgAlB_{14}$, $ErAlB_{14}$). Optical absorption spectra, in particular in the range of the absorption edge [93W].

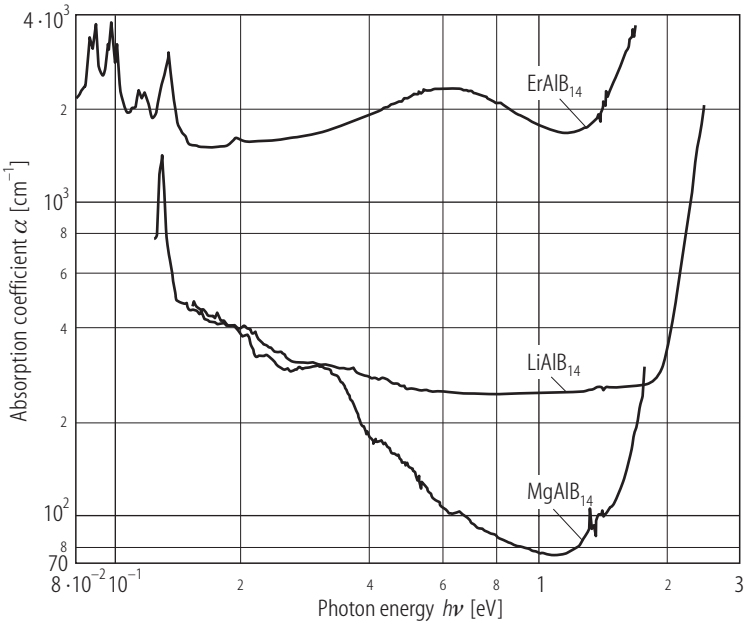

**Fig. 3.**

$MgAlB_{14}$ type orthorhombic structure group ($LiAlB_{14}$, $MgAlB_{14}$). Reflectivity spectra [93W].

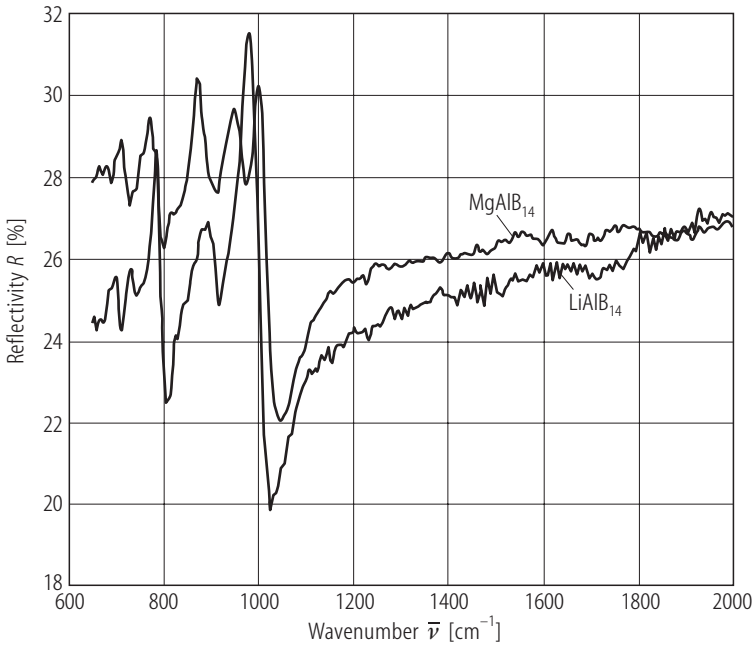

**Fig. 4.**

$MgAlB_{14}$ type orthorhombic structure group ($LiAlB_{14}$ (left ordinate), $ErAlB_{14}$ (right ordinate)). Optical absorption spectra in the range of single atom vibrations [93W].

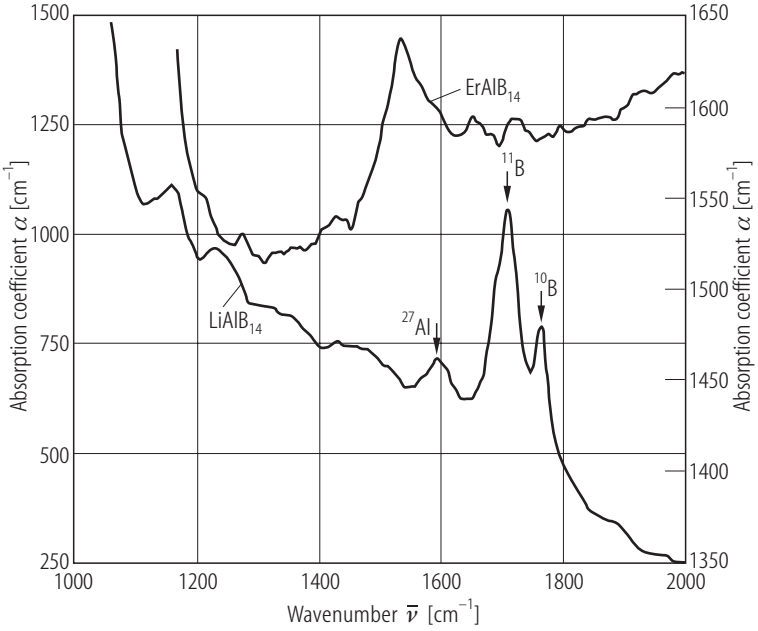

**Fig. 5.**

$MgAlB_{14}$. Electrical conductivity vs. reciprocal temperature for polycrystalline samples. Curve *1*: pure $MgAlB_{14}$; curve *2*: $MgAlB_{14}$ (nickel alloyed) [79B].

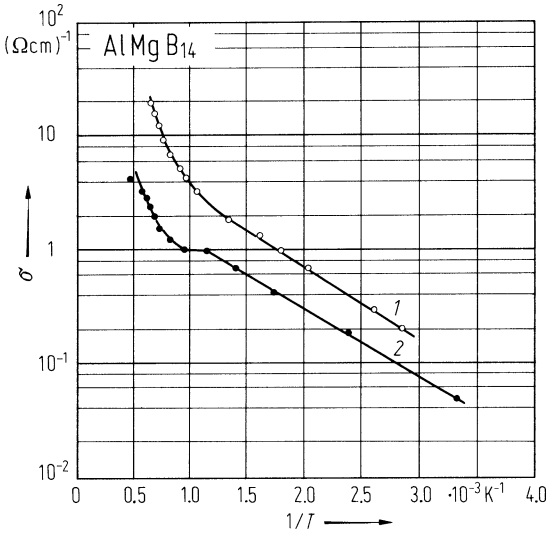

**Fig. 6.**

$MgAlB_{14}$. Temperature dependence of the electrical conductivity; *(1)* undoped; *(2)* Fe-doped ($Fe(MgAlB_{14})_{30}$ [89K

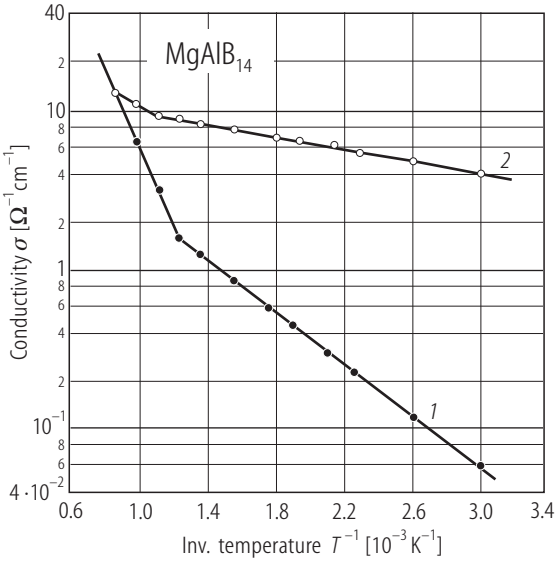

**Fig. 7.**

$MgAlB_{14}$. Thermoelectric power vs. temperature for polycrystalline samples Curve *1*: pure $MgAlB_{14}$; curve *2*: $AlMgB_{14}$ (nickel alloyed) [79B].

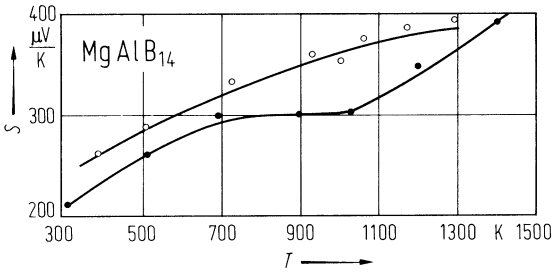

**Fig. 8.**

$MgAlB_{14}$. Thermoelectric power vs. carrier concentration determined by Hall effect [87G].

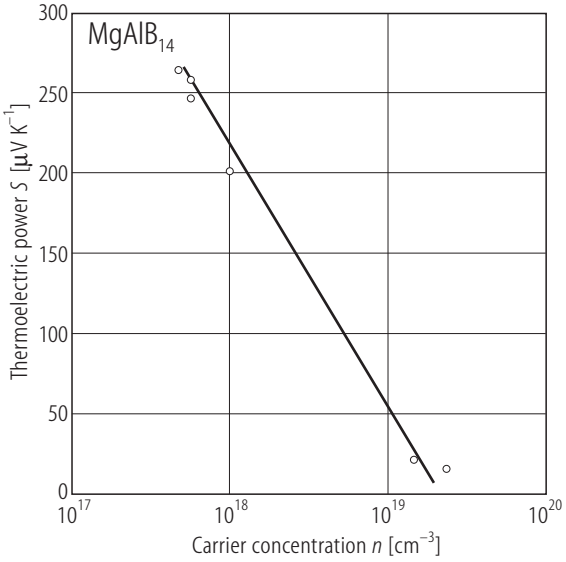

**Fig. 9.**

$MgAlB_{14}$. Temperature dependence of the thermoelectric power; *(1)* undoped; *(2)* Fe-doped ($Fe(MgAlB_{14})_{30}$ [89K].

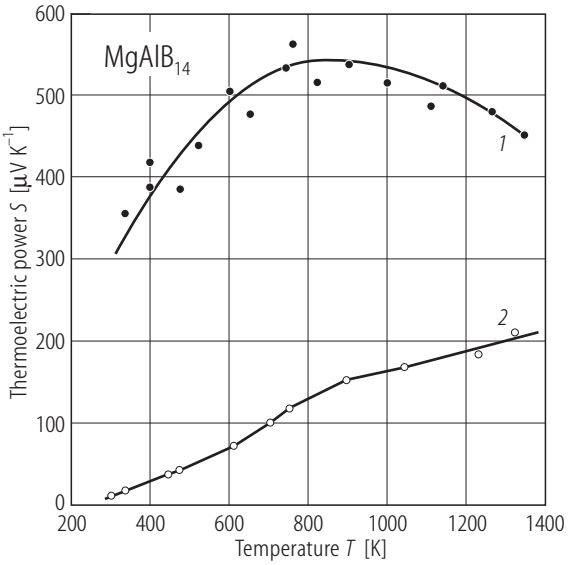

**Fig. 10.**

$MgAlB_{14}$:Ni. Electrical conductivity and thermoelectric power vs. reciprocal temperature [83G]. Ni concentration not specified.

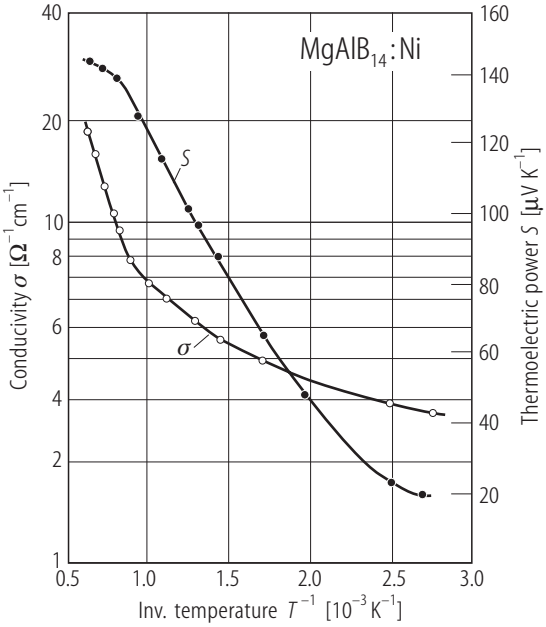

**Fig. 11.**

$MgAlB_{14}$ :Fe. Thermoelectric power vs. reciprocal temperature for undoped, 0.5 at.% Fe, 2 at.% Fe doped samples [94G].